

Morphology-Controlled $\text{CH}_3\text{NH}_3\text{PbI}_3$ Films by Hexane-Assisted One-Step Solution Deposition for Hybrid Perovskite Mesoscopic Solar Cells with High Reproducibility

Na Lin, Juan Qiao*, Haopeng Dong, Fusheng Ma, Liduo Wang

Key Lab of Organic Optoelectronics and Molecular Engineering of Ministry of Education, Department of Chemistry, Tsinghua University, Beijing 100084, P. R. China

Corresponding author: * Email: qjuan@mail.tsinghua.edu.cn; Fax: +86-10-62795137

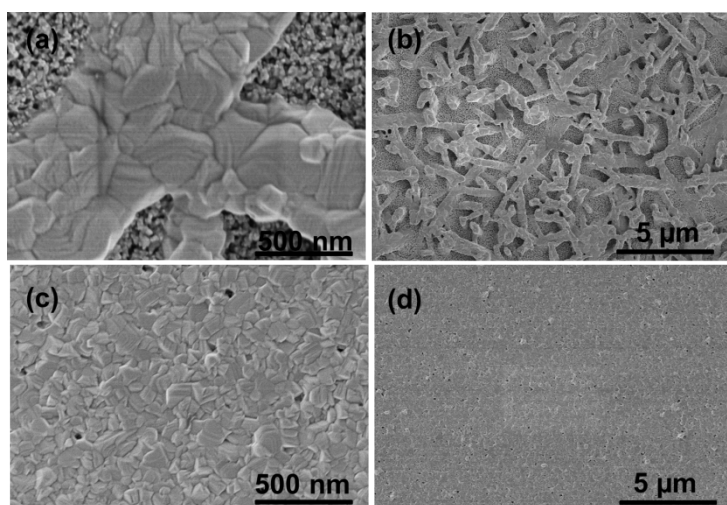


Figure S1. Typical SEM images of $\text{CH}_3\text{NH}_3\text{PbI}_3$ perovskite spin-coated on mesoporous- TiO_2 layer by (a-b) conventional and (c-d) *n*-hexane-assisted one-step solution deposition.

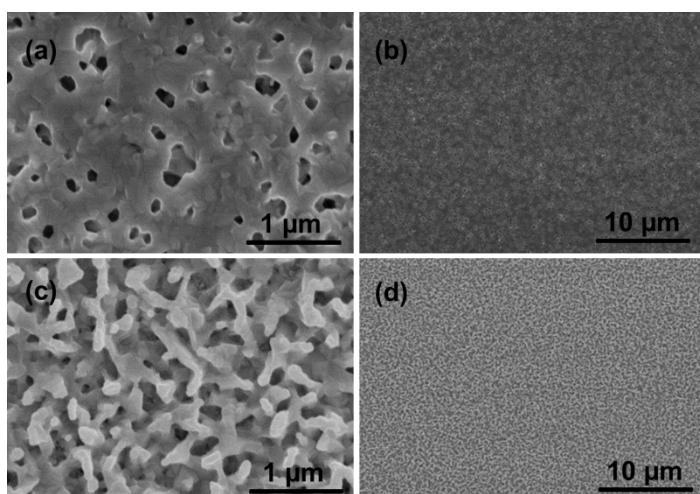


Figure S2. Typical SEM images of $\text{CH}_3\text{NH}_3\text{PbI}_3$ perovskite spin-coated on compact TiO_2 layer by dripping *n*-hexane at different delay times from the start of the spin coating process. (a-b) 6~8s; (c-d) 12~14s.

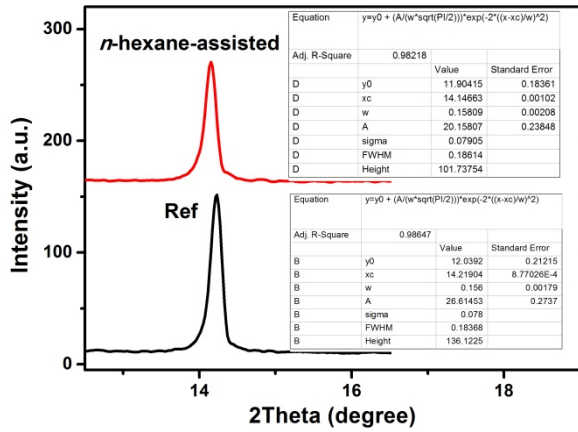


Figure S3. Comparison of crystallinity for perovskite films prepared by conventional and *n*-hexane-assisted one-step solution deposition. Full width half at maximum values of the (110) diffraction peak at 14.2 ° were obtained by Gaussian fit.

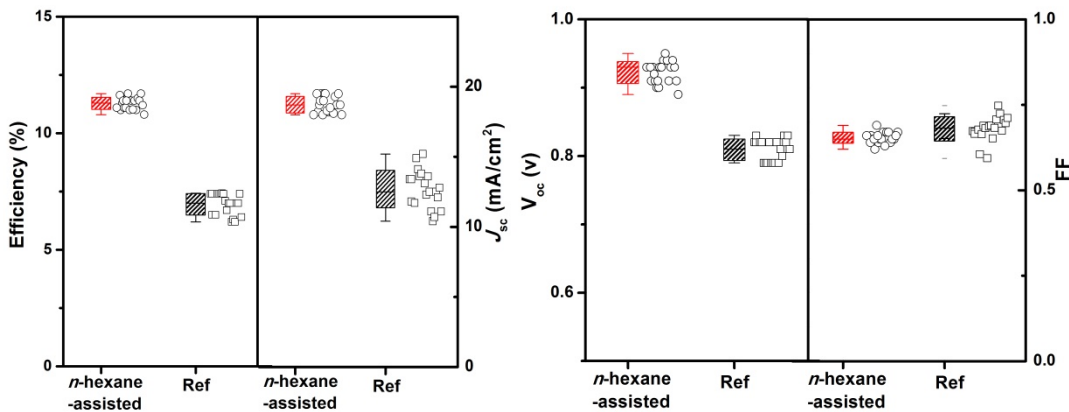


Figure S4. Box plots of the device performance parameters of FTO/c-TiO₂/m-TiO₂/CH₃NH₃PbI₃/Spiro-OMeTAD/Au devices with and without *n*-hexane dripping during the CH₃NH₃PbI₃ perovskite deposition process.

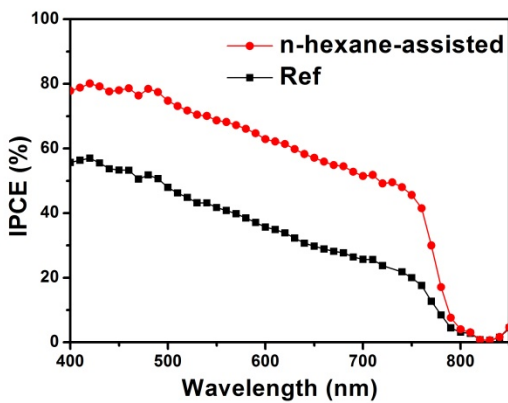


Figure S5. The IPCE of FTO/c-TiO₂/ m-TiO₂/CH₃NH₃PbI₃/Spiro-OMeTAD/Au devices with and without *n*-hexane

dripping during the $\text{CH}_3\text{NH}_3\text{PbI}_3$ perovskite deposition process.

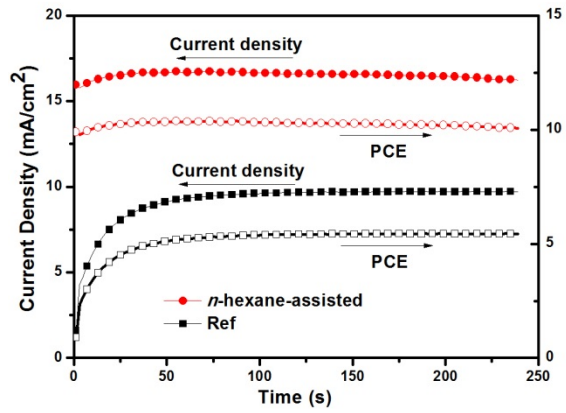


Figure S6. Photocurrent density and power conversion efficiency as a function of time for the FTO/c-TiO₂/ m-TiO₂/CH₃NH₃PbI₃/Spiro-OMeTAD/Au cells with and without hexane-assisted solution deposition process held close to 0.58 V and 0.62 V forward bias respectively.

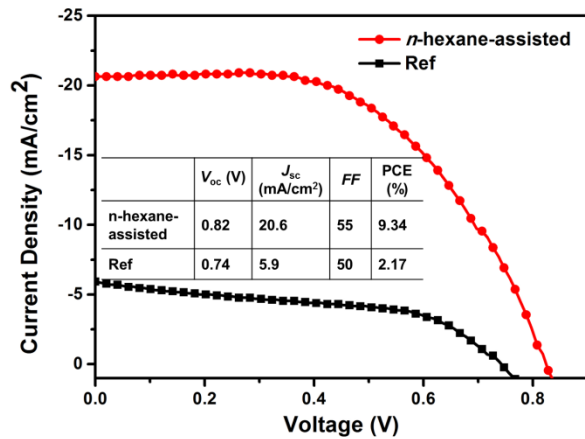


Figure S7. The J - V characteristics of FTO/c-TiO₂/CH₃NH₃PbI₃/Spiro-OMeTAD/Au solar cells with and without hexane-assisted solution deposition process.

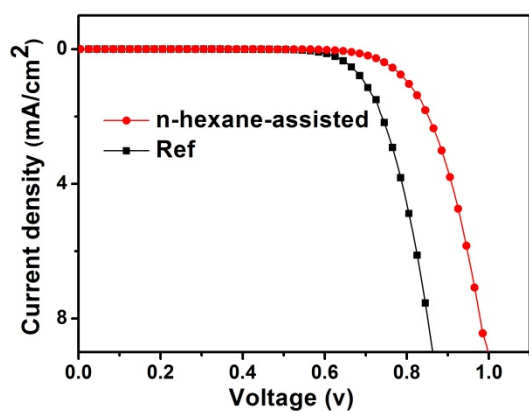


Figure S8. The dark current curves of devices with and without *n*-hexane dripping during the $\text{CH}_3\text{NH}_3\text{PbI}_3$ perovskite deposition process.

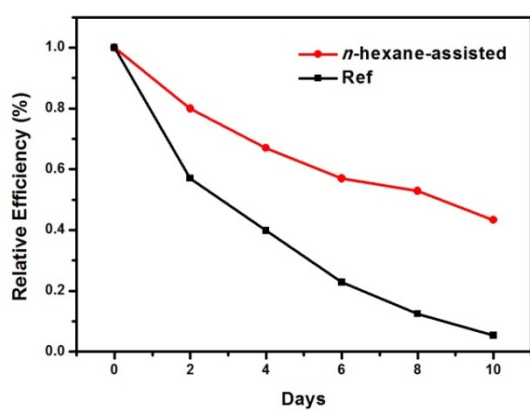


Figure S9. Relative efficiencies of perovskite solar cells versus time stored in air at room temperature under about 50% humidity without encapsulation, in which the perovskite films are fabricated with and without *n*-hexane dripping during the $\text{CH}_3\text{NH}_3\text{PbI}_3$ deposition process.